Revisiting Lighthill's acoustic analogy

Manfred Kaltenbacher[1,2], Stefan Schoder[1]
[1] Institute of Mechanics and Mechatronics, TU Wien, Austria
Email: manfred.kaltenbacher@tuwien.ac.at, stefan.schoder@tuwien.ac.at
[2] Institute of Fundamentals and Theory in Electrical Engineering, TU Graz, Austria
Email: manfred.kaltenbacher@tugraz.at

Introduction

Lighthill's analogy is an exact reformulation of the fluid dynamic equations into an inhomogeneous wave equation. Thereby, the source term not only accounts for the generation of sound but also acoustic non-linearity, convection, and refraction of sound waves by the flow, as well as attenuation due to thermal and viscous actions. To compute the flow-induced sound, one needs Lighthill's tensor for which the full set of compressible flow dynamics equations have to be solved. However, for low Mach number flows, the Reynolds stress tensor is the leading order term, which can be obtained by an incompressible flow computation. Furthermore, we want to note that Lighthill's inhomogeneous wave equation with the physical correct boundary conditions can be applied to any aeroacoustic application and the second spatial derivative of Lighthill's tensor contains all physical aeroacoustic source terms.

Lighthill's analogy

Historically, the proposed acoustic analogy by Lighthill [1, 2] transformed the compressible flow equations into an exact inhomogeneous wave equation, without any physical approximation and assumptions to boundaries. Lighthill's inhomogeneous wave in terms of the fluctuating density ρ' reads as

$$\frac{\partial^2}{\partial t^2}\rho' - c^2\nabla\cdot\nabla\rho' = \nabla\cdot\nabla\cdot\mathbb{T}\,. \tag{1}$$

In (1), Lighthill's tensor $\mathbb{T}$ represents all remaining terms when rearranging mass and momentum equations

$$\mathbb{T} = \rho\boldsymbol{u}\boldsymbol{u} - \mathbb{S} + p'\mathbb{I} - c^2\rho'\mathbb{I}\,. \tag{2}$$

In (2) $\boldsymbol{u}$ denotes the flow velocity, $\mathbb{S}$ the viscous stress tensor, p' the pressure fluctuation, $\mathbb{I}$ the unit tensor, and c the speed of sound. Please note that the terms in $\mathbb{T}$ not only account for the generation of sound, but also include acoustic nonlinearity, the convection of sound waves by the turbulent flow velocity, refraction caused by sound speed variations and attenuation due to thermal and viscous actions [3]. Lighthill proposed the solution of (2) by using Green's function for free field radiation. The obtained integral equation is defined by

$$c^2\rho'(\boldsymbol{x},t) = \frac{1}{4\pi}\int_{-\infty}^{\infty}\frac{\partial^2 T_{ij}(\boldsymbol{y},t-|\boldsymbol{x}-\boldsymbol{y}|/c_0)}{\partial x_i\partial x_j}\frac{\mathrm{d}\boldsymbol{y}}{|\boldsymbol{x}-\boldsymbol{y}|} \tag{3}$$

with the source coordinate $\boldsymbol{y}$ and $\boldsymbol{x}$ the coordinate at which the density fluctuation is computed. In (3), also know als Lighthill's integral formulation, the term $\partial^2 T_{ij}/\partial x_i\partial x_j$ may be interpreted as a quadrupole, due to the use of Green's function for free radiation. In doing so, resonators and bodies in the neighborhood of the sources as well as diffraction, scattering, absorption, and reflection by solid boundaries are neglected. Curle [4] investigated the effects of surfaces at rest in the context of the integral solution of Lighthill's theory. Surfaces at rest are equivalent to a surface dipole distribution. Ffowcs Williams and Hawkings [5] extended Kirchhoff's formula [6] and generalized the integral solution towards accounting for arbitrary moving bodies in the source domain. The second approach focuses on the solution of Lighthill's inhomogeneous wave equation by a volume discretization method (e.g., Finite-Volume method, Finite-Element method, etc.) equipped with appropriate boundary conditions, see e.g. [7, 8, 9, 10, 11]. In doing so, the interpretation of Lighthill's source term being the right hand side of (1) as a quadrupole type term is physically wrong because the boundary conditions specify the radiation pattern. In [12] it was successfully demonstrated that the surface distribution of Curle's analogy is equivalent to the scattering of sound waves by the rigid surface, which is originally generated by the volume distribution of quadrupoles (second spatial derivative of Lighthill's tensor).

In summary, the whole set of compressible flow dynamics equations have to be solved in order to be able to calculate Lighthill's tensor and therefore the right-hand side of (1). However, this means that we have to resolve both the flow structures and acoustic waves, which is an enormous challenge for any numerical scheme and the computational noise itself may strongly disturb the physical radiating wave components [13]. Therefore, in the theories of Phillips and Lilley interaction effects have been, at least to some extend, moved to the wave operator [14, 15]. These equations predict certain aspects of the sound field, surrounding a jet, quite accurately. These aspects are not accounted for Lighthill's equation (1), due to the restricted numerical resolution of the source term.

Lighthill's analogy for low Mach number

For practical applications of Lighthill's analogy, it is beneficial to know the leading order term of Lighthill's tensor. This analysis has been done in [16] for low Mach number flows in an isentropic medium by applying the

method of matched asymptotic expansion (see, e.g., [13]). Sound emission from vortical flow structures involves three length scales: the eddy size l, the wavelength λ of the sound, and a dimension L of the region. The problem is solved for $\mathrm{Ma} \ll 1$ and $L/l \sim 1$ by matching the compressible eddy core scaled by l to a surrounding acoustic field scaled by λ. Thereby, Lighthill's solution is shown to be adequate in both regions, if T_{ij} is approximated by

$$T_{ij} \approx \rho_0 u_{\mathrm{ic},i} u_{\mathrm{ic},j} \tag{4}$$

with $\boldsymbol{u}_{\mathrm{ic}}$ the incompressible flow velocity. Such a flow field is described by solving the incompressible fluid dynamics equations. Thereby, we obtain an incompressible flow velocity $\boldsymbol{u}_{\mathrm{ic}}$ and pressure p_{ic}. Since for incompressible flows, the divergence of $\boldsymbol{u}_{\mathrm{ic}}$ is zero, we may rewrite the second spatial derivative of (4) by

$$\frac{\partial^2}{\partial x_i x_j}\left(\rho_0 u_{\mathrm{ic},i} u_{\mathrm{ic},j}\right) = \rho_0 \frac{\partial u_{\mathrm{ic},j}}{\partial x_i} \frac{\partial u_{\mathrm{ic},i}}{\partial x_j} \,. \tag{5}$$

Furthermore, applying the divergence to the conservation of momentum provides the following equivalence (using $\nabla \cdot \boldsymbol{u}_{\mathrm{ic}} = 0$) [17]

$$\nabla \cdot \nabla p_{\mathrm{ic}} = -\rho_0 \frac{\partial^2 u_{\mathrm{ic},i} u_{\mathrm{ic},j}}{\partial x_i \partial x_j} \,. \tag{6}$$

With such an approach, we totally separate the flow from the acoustic field, which also means that any influence of the acoustic field on the flow field is neglected. Thereby, we arrive at the following subset of Lighthill's equation

$$\frac{1}{c^2}\frac{\partial^2 p'}{\partial t^2} - \nabla \cdot \nabla p' = \nabla \cdot \nabla p_{\mathrm{ic}} \tag{7}$$

for the fluctuating pressure p'. Here, we have assumed an isentropic fluid state relating the density fluctuation ρ' with the pressure fluctuation p' via the speed of sound c. Applying a decomposition of the fluctuating pressure p' in its incompressible part p_{ic} and its acoustic part p_{a} via

$$p' = p_{\mathrm{ic}} + p_{\mathrm{a}}$$

transforms (7) into

$$\frac{1}{c^2}\frac{\partial^2 p_{\mathrm{a}}}{\partial t^2} - \nabla \cdot \nabla p_{\mathrm{a}} = \frac{-1}{c^2}\frac{\partial^2 p_{\mathrm{ic}}}{\partial t^2} \,, \tag{8}$$

which was named AWE (Aeroacoustic Wave Equation) [18]. Thereby, (8) is equivalent to Ribner's dilatation equation [19], who reformulated the fluctuating density ρ' of Lighthill's analogy via

$$c^2 \rho' = p' = p_0 + p_{\mathrm{a}}$$

and named p_0 the pseudo part. For further discussion and a comprehensive overview, we refer to [20].

Application

As a first demonstrative example, we choose a cylinder in a cross-flow, as displayed in Fig. 1. Thereby, the computational grid is just up to the height of the cylinder

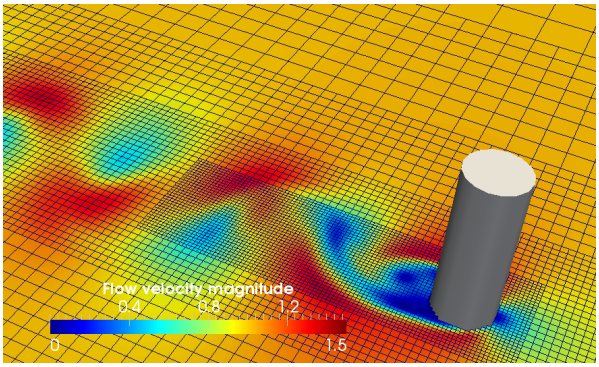

Figure 1: Computational setup for flow computation.

and together with the boundary conditions (bottom and top as well as span-wise direction symmetry boundary condition), we obtain a pseudo two-dimensional flow field. The diameter of the cylinder D is 1 m resulting with the inflow velocity of 1 m/s and chosen viscosity in a Reynolds number of 250 and Mach number of 0.2. From the flow simulations, we obtain a shedding frequency of 0.2 Hz (Strouhal number of 0.2). The acoustic mesh is chosen different from the flow mesh, and resolves the wavelength of two times the shedding frequency with 10 finite elements of second order. At the outer boundary of the acoustic domain we add a perfectly matched layer to efficiently absorb the outgoing waves. For the acoustic

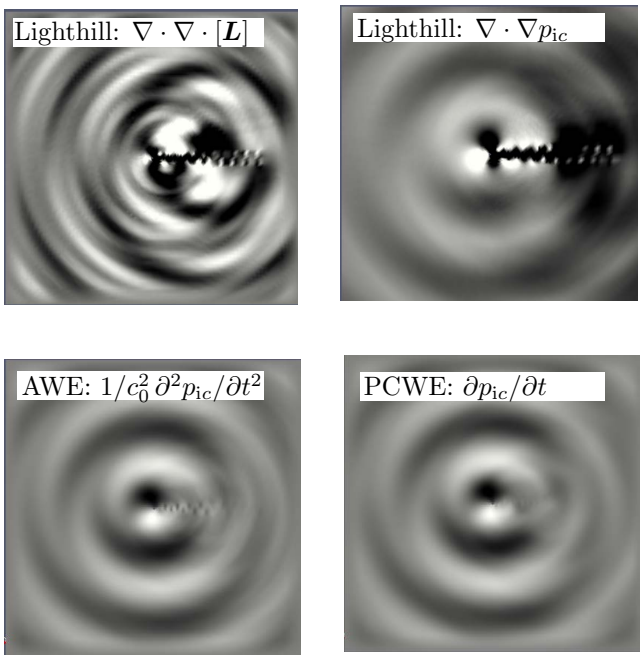

Figure 2: Computed acoustic field (in case of PCWE and AWE) and pressure fluctuation (in case of Lighthill) with the different formulations.

field computation we use the following formulations:

- Lighthill's acoustic analogy with Lighthill's tensor $\mathbb{T}$ according to (4) as source term

- Lighthill's acoustic analogy with the Laplacian of

the incompressible flow pressure p_{ic} as source term (see (7))

- the aeroacoustic wave equation (AWE) according to (8)

- Perturbed Convective Wave Equation (PCWE) [21], which is an exact reformulation of the acoustic perturbation equations for low Mach number [22]; for comparison, we set the mean flow velocity $\bar{\boldsymbol{v}}$ to zero.

Figure 2 displays the acoustic field / pressure fluctuations for the different formulations. One can clearly see that the acoustic field of PCWE (for comparison with the other formulations we have neglected the convective terms) meets very well the expected dipole structure and is free from dynamic flow disturbances. Furthermore, the acoustic field of AWE is quite similar and exhibits almost no dynamic flow disturbances. Both computations with Lighthill's analogy show flow disturbances, whereby the formulation with the Laplacian of the incompressible flow pressure as source term shows qualitative better result as the classical formulation based on the incompressible flow velocities. Please note that the solution of Lighthill's inhomogeneous wave equation according to (1) with (4) as well as (7) results in the pressure fluctuation p', which includes both the aerodynamic flow pressure fluctuation and the acoustic pressure. Therefore, one has to evaluate p' outside the flow region to obtain the acoustic pressure p_{a}. Please consider that due to the restrictions of numerical schemes the solution of p' in the far field may result in a disturbed acoustic pressure p_{a}.

The second example performs aeroacoustic computations of the human voice. Thereby, the incompressible flow is computed for the larynx (see Fig. 4) [23]. The geometry of the vocal folds are modeled according to the "M5" model with a medial surface convergence angle of $\psi = -20°$. To simulate the vocal folds oscillation a sinusoidal motion is prescribed in inferior and superior direction, given by

$$w \quad = \quad A \sin(2\pi f). \tag{9}$$

Thereby, a frequency of $f = 100$ Hz and a oscillation amplitude of $A = 4$ mm is used, ensuring that the minimal gap between the two vocal folds of $g = 0.2$ mm is kept [23].

For the acoustics, the vocal tract model is attached to the larynx and consists of multiple frustums concatenated one after another. The number of frustums and their radius determines the resulting sound radiating from the artificial mouth, and the case models the vocal tract for /u/ ("who").

For the evaluation of the acoustic pressure and the comparison of the hybrid approaches, two monitoring points are considered. The first "MIC 1" is situated at the end of the larynx, inside the flow domain. "MIC 2", the second monitoring point, is 1 cm behind the vocal tract, in

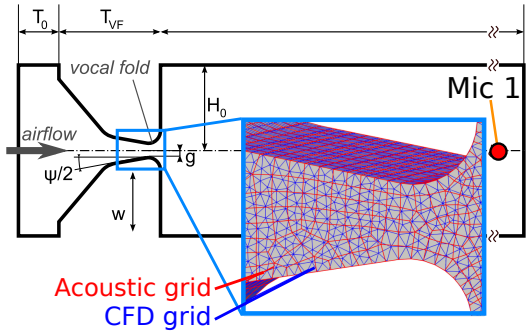

Figure 3: Geometric model of the human larynx in coronal section. Comparison of the fine CFD grid and coarse acoustic grid.

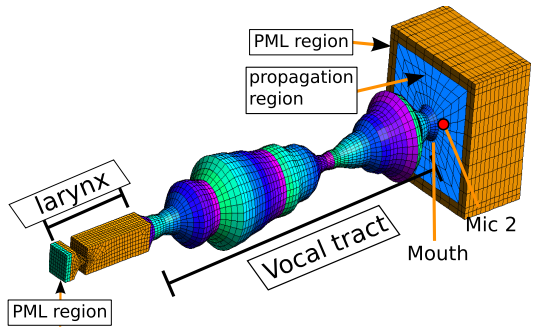

Figure 4: Larynx, vocal tract, propagation region, perfectly matched layer (PML) regions.

the acoustic propagation region (see Fig. 4). For these two monitoring points the spectra of pressure fluctuation (in case of Lighthill) and acoustic pressure (in case of PCWE) are plotted in Fig. 5 and Fig. 6. As expected, Lighthill's approach based on the fluctuation pressure p' has significantly stronger amplitudes inside the flow region, as evident in Fig. 5. Comparing the splitting of the field quantities, between Lighthill's approach and the PCWE approach, it is clear that the resulting pressure solving (6) is superimposed by the incompressible flow pressure p^{ic}. By theory, this superimposition does not propagate into the far field as Fig. 6 shows. However, due to numerical restrictions, Lighthill's wave equation also shows some over-prediction of the SPL.

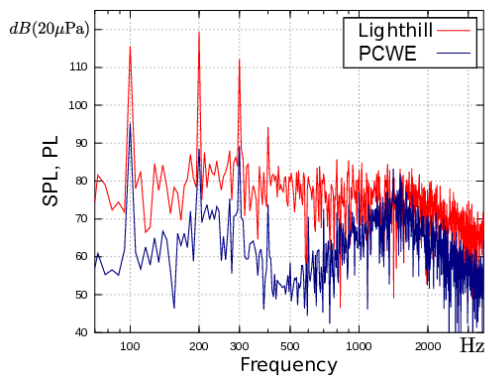

Figure 5: Spectra of pressure fluctuation (in case of Lighthill denoted by PL) and acoustic sound pressure SPL (in case of PCWE) at position Mic 1.

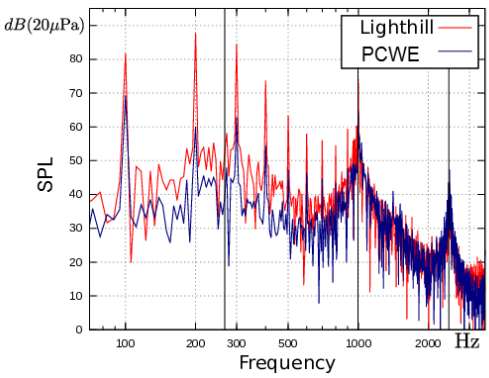

Figure 6: Spectra of obtained acoustic sound pressure SPL both for Lighthill and PCWE at position Mic 2 (outside the flow region).

References

[1] M. J. Lighthill. On sound generated aerodynamically I. General theory. *Proceedings of the Royal Society of London*, 211:564–587, 1951.

[2] M. J. Lighthill. On sound generated aerodynamically II. Turbulence as a source of sound. *Proceedings of the Royal Society of London*, 222:1–32, 1953.

[3] C. Bogey, X. Gloerfelt, and C. Bailly. Illustration of the inclusion of sound-flow interactions in Lighthill's equation. *AIAA Journal*, 41(8):1604–1606, 2003.

[4] N. Curle. The Influence of Solid Boundaries upon Aerodynamic Sound. *Proceedings of the Royal Society of London A: Mathematical, Physical and Engineering Sciences*, 231(1187):505–514, 1955.

[5] J. E. Ffowcs Williams and D. L. Hawkings. Sound Generation by turbulence and surface in arbitratry motion. *Philosophical Transactions of the Royal Society of London, Series A, Mathematical and Physical Sciences*, 264:321–342, 1969.

[6] W. R. Morgan. The Kirchhoff Formula Extended to a Moving Surface. *Philosophical Magazine*, 9:141–161, 1930.

[7] A. Oberai, F. Roknaldin, and T. Hughes. Computation of trailing-edge noise due to turbulent flow over an airfoil. *AIAA journal*, 40(11):2206–2216, 2002.

[8] R. M. A. Marretta and G. Tassone. A vorticity based aeroacoustic prediction for the noise emission of a low-speed turbulent internal flow. *Computers & fluids*, 32(4):457–478, 2003.

[9] M. Kaltenbacher, M. Escobar, S. Becker, and I. Ali. Computational aeroacoustics based on Lighthill's acoustic analogy. In *Computational Acoustics of Noise Propagation in Fluids-Finite and Boundary Element Methods*, pages 115–142. Springer, 2008.

[10] S. Caro, Y. Detandt, J. Manera, F. Mendonca, and R. Toppinga. Validation of a New Hybrid CAA Strategy and Application to the Noise Generated by a Flap in a Simplified HVAC Duc. In *15th AIAA/CEAS Aeroacoustics Conference*, 2009-3352, 2009.

[11] M. Kaltenbacher, M. Escobar, I. Ali, and S. Becker. Numerical Simulation of Flow-Induced Noise Using LES/SAS and Lighthill's Acoustics Analogy. *International Journal for Numerical Methods in Fluids*, 63(9):1103–1122, 2010.

[12] X. Gloerfelt, F. Pérot, C. Bailly, and D. Juvé. Flow-induced cylinder noise formulated as a diffraction problem for low mach numbers. *Journal of Sound and Vibration*, 287(1):129 – 151, 2005.

[13] D. G. Crighton, A. P. Dowling, J. E. Ffowcs-Williams, M. Heckl, and F. G. Leppington. *Modern methods in analytical acoustics*. Springer Lecture Notes, 1992.

[14] O. M. Phillips. On the generation of sound by supersonic turbulent shear layers. *Journal of Fluid Mechanics*, 9(1):1–28, 1960.

[15] G. M. Lilley. *On the noise from jets*. AGARD-CP-131, 1974.

[16] S. C. Crow. Aerodynamic sound emmission as a singular perturbation problem. *Studies of Applied Mathematics*, 49:21–44, 1970.

[17] M. Kaltenbacher. *Computational Acoustics*. CISM International Centre for Mechanical Sciences. Springer International Publishing, 2017.

[18] M. Kaltenbacher and A. Hüppe. Comparison of aeroacoustic source term formulations. In *DAGA*, 2014.

[19] H. S. Ribner. Aerodynamic Sound from Fluid Dilatations - A Theory of the Sound from Jets and Other Flows. Technical report, Institute for Aerospace Studies, University of Toronto, 1962.

[20] Stefan Schoder and Manfred Kaltenbacher. Hybrid Aeroacoustic Computations: State of Art and New Achievements. *Journal of Theoretical and Computational Acoustics*, 27(04), 2019.

[21] M. Kaltenbacher, A. Hüppe, A. Reppenhagen, F. Zenger, and S. Becker. Computational aeroacoustics for rotating systems with application to an axial fan. *AIAA journal*, pages 3831–3838, 2017.

[22] R. Ewert and W. Schröder. Acoustic perturbation equations based on flow decomposition via source filtering. *Journal of Computational Physics*, 188(2):365–398, 2003.

[23] Petr Sidlof, Stefan Zörner, and Andreas Hüppe. A hybrid approach to the computational aeroacoustics of human voice production. *Biomechanics and Modeling in Mechanobiology*, 2014.